

RUSSIAN ACADEMY OF SCIENCE
FERSMAN MINERALOGICAL MUSEUM

volume 42

New Data on Minerals

FOUNDED IN 1907

MOSCOW
2007



FERROSKUTTERUDITE¹, NICKELSKUTTERUDITE, and SKUTTERUDITE FROM THE NORILSK ORE FIELD

Ernst M. Spiridonov

Lomonosov Moscow State University, Moscow, mineral@geol.msu.ru

Yulia D. Gritsenko

Lomonosov Moscow State University, Moscow, mineral@geol.msu.ru

Co-Ni-Fe triarsenides skutterudite, nickelskutterudite and ferroskutterudite have been identified in the Norilsk ore field for the first time. They are hosted in the apophyllite – anhydrite – dolomite – calcite metamorphic hydrothermal veins that occur within the proximal zone of the magmatic Co-Ni-Cu sulfide ores, which have been affected by epigenetic prehnite-pumpellyite and zeolite facies metamorphism. The Co-Ni-Fe triarsenides have overgrown the Co-Ni diarsenide segregations with which they form complex intergrowths. Both skutterudite and nickelskutterudite, and skutterudite and ferroskutterudite, from Norilsk form continuous isomorphic series. Clear negative correlation between Ni and Fe and strong positive correlation between Co and Fe and Co and S have been identified.

6 tables, 12 figures, 25 references.

A wide range of isomorphic substitutions of Fe-Co-Ni is characteristic of the iron, cobalt and nickel chalcogenides, including sulfides, sulfoarsenides, arsenides and other compounds. Frequently, there are continuous series of solid solutions including disulfides: pyrite – vaesite NiS_2 – cattierite CoS_2 , diarsenides: safflorite CoAs_2 – rammelsbergite NiAs_2 – loellingite FeAs_2 (Krutov, 1959; Shishkin, 1973; Vaughan & Craig, 1978; Vinogradova, 2002; Gritsenko & Spiridonov, 2005a). Currently, triarsenides skutterudite CoAs_3 – nickelskutterudite NiAs_3 – ferroskutterudite $(\text{Fe,Co})\text{As}_3$ are attributed to them. The continuous skutterudite-nickelskutterudite series has been described previously (Godovikov, 1959; Roseboom, 1962; Radcliffe, 1968; Petruk *et al.*, 1971; Rudashevsky *et al.*, 1975, 1976; Vaughan & Craig, 1978; Vinogradova, 2002; Fanlo *et al.*, 2004).

The skutterudite-group minerals, MeAs_3 , crystallize at low sulfur activity from hydrothermal fluids and are the As-richest arsenides of Co-Ni-Fe. Therefore, they are probably deposited in carbonate veins, whereas the As-depleted maucherite, $\text{Ni}_{11}\text{As}_8$, and niccolite, NiAs , are common in hydrothermally altered peridotite, basic rocks, and metamorphosed Cu-Ni sulfide ores.

Arsenide mineralization occurs in metamorphosed Ni-Cu sulfide ores (Schneiderhöhn, 1955; Yakovlev *et al.*, 1981; Hytönen, 1999;

Spiridonov *et al.*, 2000; Gritsenko & Spiridonov, 2005a, 2005b, 2006). The skutterudite-group minerals are characteristic of Co-Ni-Ag-Bi-U deposits and Ni-Co arsenide deposits (Schneiderhöhn, 1955; Krutov, 1959; Petruk *et al.*, 1971; Shishkin, 1973; Rudashevsky *et al.*, 1975, 1976; Fanlo *et al.*, 2004).

NORILSK ORE FIELD

The Norilsk ore field is located in the plate cover of the Pre-Rephean East Siberian Platform within the zone of marginal deformation. The Co-Ni-Cu magmatic ores of the 250 ± 5 Ma age are related to the gabbrodolerite intrusions of the Upper Permian to Lower Triassic trap assemblage (Godlevsky, 1959; Dodin *et al.*, 1971; Genkin *et al.*, 1981). Magmatic sulfides are disseminated near the base (and at some other levels) of the Norilsk, Talnakh and Taimyr plutons and form massive orebodies, veins and impregnations, mainly in the lower near-contact igneous rocks and adjacent wall rocks. The Norilsk-1 deposit is exploited by the Zapolyarny, Medvezhy Ruchi, and Ugol'ny Ruchi Mines; the Talnakh deposit, Mayak, Komsomol'sky, and Skalisty mines; Taimyr (Oktyabr'sky), Oktyabr'sky and Komsomol'sky mines.

The primary ores are composed of segregations of pyrrhotite- and chalcopyrite-group minerals, cubanite and pentlandite (which are the result of solid-state modifications of Mss and Iss crystallized from sulfide melts) and

¹ A new mineral ferroskutterudite and its name were approved by the Commission on New Minerals and Mineral Names, International Mineralogical Association, October 24, 2006. The type ferroskutterudite is deposited in the Fersman Mineralogical Museum, Russian Academy of Sciences, Moscow. Registration number is 3440/1

magnetite. The composition of the primary ores ranges from pentlandite-troilite-pyrrhotite through pentlandite-pyrrhotite-cubanite and pentlandite-cubanite-talnakhite to pentlandite-chalcopryrite (Godlevsky, 1959; Kulagov, 1968; Genkin *et al.*, 1981). During post-intrusion fluid conversion, magmatic sulfides recrystallized and minerals of Pd, Pt, Au and Ag formed (Spiridonov *et al.*, 2004).

Areas of the East Siberian Platform are covered by thick sequences of basalt and tuff, and are intruded by numerous dolerite and gabbrodolerite plutons of the trap assemblage. The trap assemblage and lower sequences were affected by the 3-generation regional metamorphism. Generation-1 involved the zeolite facies (Rb/Sr age estimated from apophyllite is 232 to 212 Ma), generation-2, zeolite to prehnite-pumpellyite facies (Rb/Sr age estimated from apophyllite and metabasalt as whole rock is of 212 to 196 Ma), and generation 3, high- to low-temperature part of the zeolite facies (Rb/Sr age estimated from apophyllite is of 212 to 196 Ma) (Spiridonov *et al.*, 2000). The copper-zeolite assemblage, Iceland spar and zeolite deposits, agate and datolite mineralization, and barite, celestine, and (Zn, Pb, Cu, and Ag)-sulfide occurrences are related to this metamorphism (Fig. 1).

The Norilsk ore-bearing plutons and sulfide ores were also affected by low-grade metamorphism. Metadolerite contains prehnite, pumpellyite, epidote, albite, potassium feldspar, titanite,

chlorite and serpentine-group minerals, carbonate, hydrogarnet, actinolite, grunerite, seladonite, ilvaite, diverse zeolites, apophyllite, xonotlite, pectolite, datolite, okenite and thaumasite. The metamorphosed sulfide ores contain pyrite, Ni-pyrite, valleriite, acicular bornite, millerite, heazlewoodite, chalcocite, mackinawite, hematite, ilvaite, violarite, godlevskite, cobaltpentlandite, tochilinite, vyalsovite, and arsenides and antimonides of Ni and Co (Spiridonov *et al.*, 2000). Typical paragenetic associations of the metamorphosed ores are Ni-pyrite + magnetite + valleriite, chalcopryrite + millerite + pyrite, bornite + millerite, and chalcocite + heazlewoodite. Segregations of bornite are cut, overgrown and replaced by segregations of chalcocite.

Antimonide-arsenide mineralization

Metamorphic hydrothermal impregnated and vein mineralization is prominent in the joint zones adjacent to tectonic faults, especially in the zone of the large Norilsk-Kharaelakh fracture, as well as in sedimentary rocks enriched in anhydrite and clay minerals. Ni, Co and Fe arsenides and Ni antimonides are disseminated in metamorphosed Co-Ni-Cu sulfide ores and form pods and impregnations in hydrothermal veins (Godlevsky, 1959; Kulagov, 1968; Dodin *et al.*, 1971; Izoitko & Vyal'sov, 1973; Distler *et al.*, 1975; Genkin *et al.*,

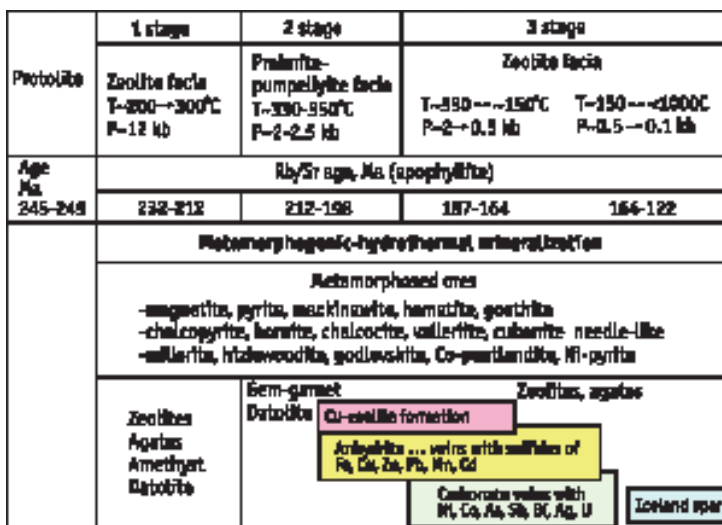


Fig. 1. Low grade metamorphic generations and their isotopic age in the Norilsk region, East Siberian Platform.

1981; Gritsenko & Spiridonov, 2005a, 2005b, 2006). The Co-Ni-Fe triarsenides were identified in the Norilsk ore field for the first time.

The chlorite-carbonate, carbonate (with prehnite and quartz), and apophyllite-anhydrite-carbonate veins with antimonides and arsenides occur at each deposit of the ore field. They are numerous at Talnakh, in the eastern part of Oktyabrsky (Komsomolsky Mine), and in the southern part of Norilsk-1 (Medvezhy Ruchei Mine). The veins of 0.3 to 150 cm thick and 0.1 to 15 m long. Calcite from the arsenide-bearing veins contains primary inclusions of NaCl-MgCl₂ fluids with high salinity ranging from 6.5 to 12.6 wt % eq NaCl. Pressure and temperature of deposition estimated from these inclusions range 0.9 to 0.1 kb and from 216 to 127°C. PT parameters of the arsenide mineralization correspond to those of zeolite-facies metamorphism. The isotopic age of apophyllite from the arsenide-bearing veins is 164 Ma, corresponding to the late generation of the burial regional metamorphism (Spiridonov *et al.*, 2002).

The calcite, calcite-dolomite and apophyllite-anhydrite-carbonate veins with the Ni-Co arsenides occur only within or adjacent to the metamorphosed deposits of Co-N-Cu ores. The calcite and anhydrite-calcite veins with native arsenic and loellingite occur both within and outside the metamorphosed deposits of sulfide ores. The metamorphosed Co-Ni-Cu sulfide ores were the source for the Co-Ni-Sb-As mineralization.

The history of the antimonide-arsenide mineralization is complex. On the basis of relations of brecciation, cross-cutting, overgrowth, and replacement, 12 mineral assemblages formed during these three generations have been recognized.

The generation-1 antimonide-arsenide mineralization is associated with bornite-bearing ore, trending from Ni monoarsenide through Ni and Co di- and triarsenide to native arsenic. Generation-1 comprises nine mineral assemblages: 1) cobaltite-gersdorffite-maucherite-Sb-niccolite-niccolite, 2) maucherite-gersdorffite-niccolite with Sb-niccolite, 3) breithauptite-maucherite, 4) loellingite-rammelsbergite-breithauptite-niccolite, 5) cobaltite-breithauptite-maucherite-Co-niccolite, 6) maucherite-breithauptite-Co-niccolite, 7) rammelsbergite-niccolite, 8) di- and triarsenide with safflorite, and

9) with native arsenic and loellingite.

The generation-2 antimonide-arsenide mineralization occurs in metamorphosed ores which are frequently enriched in chalcocite; native silver and bismuth, Hg-rich silver, pyrargyrite, clausthalite and other selenides, and uraninite are characteristic minerals. Generation-2 comprises two assemblages: niccolite-breithauptite-rammelsbergite-loellingite and Sb-niccolite-breithauptite.

The generation-3 sulfoarsenide-sulfoantimonide mineralization (latest assemblage) is associated with the pyrite- and marcasite-bearing metamorphosed ores.

The antimonide-arsenide mineralization is enriched in Ni that correlates with the composition of the Norilsk ores. Arsenides enriched in Co periodically crystallized after deposition of significant amount of Ni minerals.

Arsenides and antimonides aggregates show us so-called geometric selection patterns, indicating crystallization from normal solutions in open space.

Material and Research

More than 100 samples from carbonate veins with arsenide mineralization from all deposits of the Norilsk ore field have been studied. These samples were collected by the authors during field investigation of 1998 to 2004 and kindly placed at our disposal by geologists of the Zavenyagin Norilsk Mining and Metallurgical Company: E.A. Kulagov, S.N. Belyakov, E.V. Sereda, A.P. Glotov, and V.V. Butenko. The chemical composition of minerals was analyzed with a CAMEBAX electron microprobe, I.M. Kulikova, analyst, Institute of Geology, Geochemistry and Crystallography of Rare Elements, Russian Academy of Sciences, Moscow and with a CAMEBAX SX-50 electron microprobe, N.N. Kononkova, analyst, Division of Mineralogy, Lomonosov Moscow State University. The BSE images were made with a CAMSCAN 4DV scanning electron microscope equipped with a LINK 10000 energy-dispersion system, N.N. Korotaeva and E.V. Guseva, analysts Division of Petrology, Lomonosov Moscow State University. The X-ray diffraction patterns of skutterudite and nickelskutterudite were collected with a DRON-4.5 diffractometer, Division of Inorganic Chemistry, Lomonosov Moscow State University. Fluid inclusions in calcite from

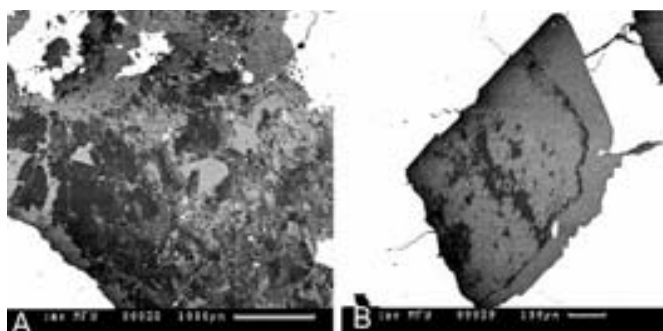


Fig. 2. BSE images of dolomite, calcite and anhydrite from the hydrothermal arsenide veins.

A) Dolomite crystals (dark grey) overgrown and partly replaced by calcite (grey). Anhedral anhydrite (light grey) fills interstices. Arsenides are white.

B) Pseudomorphs of calcite (light grey) after dolomite (dark grey). Safflorite is white.

the arsenide veins were studied in the laboratory of the Institute of Geology of Ore Deposits, Petrography, Mineralogy and Geochemistry, Russian Academy of Sciences, V.Yu. Prokof'ev and Yu.D. Gritsenko, analysts.

These analysis numbers on the figures correspond to the analyzed points in the tables.

Skutterudite, nickelskutterudite and ferroskutterudite from carbonate veins

The Co-Ni-Fe triarsenides were identified only in one of the small systems of anhydrite-calcite-dolomite veins at the South-East flank of the Taimyr ore-bearing pluton (Komsomolsky Mine). In this area, there were steeply dipping carbonate veins to 7 cm thick with irregular impregnation of arsenide segregations, as well as light sphalerite, magnetite and galena within about 2 m of the thick joint zone. The arsenide segregations are microscopic to small pods up to 21 mm cross. Sulfide and magnetite grains are less than 2 mm in size. Bluish anhydrite forms tabular crystals up to 25 x 20 x 3 mm in size and aggregates of plates or isomet-

ric grains included in milky dolomite and white or pinkish calcite. Fluor-hydroxyapophyllite and anhydrite occur in separate vein domains. Dolomite, $\text{Ca}_{1.00-1.02}\text{Mg}_{0.76-0.96}\text{Fe}_{0.03-0.15}\text{Mn}_{0.00-0.07}(\text{CO}_3)_2$, forms segregations of rhombohedral crystals 0.3 to 2 mm in size. The average composition of these dolomite is $\text{Ca}_{1.01}\text{Mg}_{0.86}\text{Fe}_{0.10}\text{Mn}_{0.03}(\text{CO}_3)_2$. Dolomite is overgrown and replaced by calcite up to entire pseudomorphs (Fig. 2). The average chemical composition of this calcite is $\text{Ca}_{0.96}\text{Mn}_{0.02}\text{Fe}_{0.01}\text{Mg}_{0.01}(\text{CO}_3)$.

Calcite-dolomite veins with Co-Ni-Fe triarsenides are composed mainly of aggregates of the 8th and to some extent 7th mineral assemblages. Fragments of niccolite up to 12 mm in size from the 7th mineral assemblage locally occur in pods of di- and triarsenides. Relic niccolite is irregularly distributed. Sb-depleted or Sb-free niccolite contains up to 0.5 wt % Co (Table 1).

Arsenides of generation-1. Niccolite is strongly corroded and overgrown by rammelsbergite-1, which in turn is partly corroded and overgrown by nickelskutterudite-1 (Figs. 3-6). Rammelsbergite-1 is characterized by blocky structure (Figs. 3B, 3C). Nickelskutterudite-1

Fig. 3. Relic niccolite in rammelsbergite-1 surrounded by nickelskutterudite-1.

A) Photomicrograph of relic niccolite (pink) in rammelsbergite-1 (light) surrounded by nickelskutterudite-1 (darker). Black veinlets are composed of calcite and anhydrite. Polished section. Width of image is 0.8 mm.

B) BSE image of relic niccolite (grey, analyses 01 and 02) in rammelsbergite-1 with different S content (light grey to dark grey, analyses 03 and 04) overgrown by nickelskutterudite-1 (white, analyses 10 and 11). Black veinlets are composed of calcite.

C) Fragment of Fig. 3B.

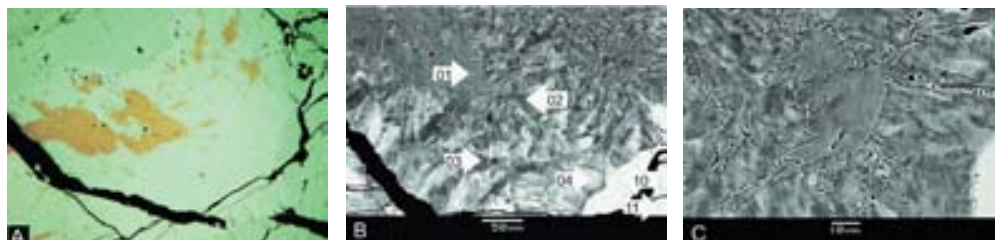


Table 1. Chemical composition of niccolite of mineral complex 7, rammelsbergite-1 and nickelskutterudite-1 of mineral complex 8 from the carbonate veins, Norilsk ore field

No anal.	Element, wt %							Formulae normalized on the basis of 2, 3, or 4 atoms									
	Ni	Co	Fe	As	Sb	S	Se	Total	Ni	Co	Fe	Total	As	Sb	S	Se	Total
									cat.							anions	
Niccolite (Fig. 3)																	
01	42.91	0.26	0.02	55.37	—	0.02	—	98.58	0.991	0.006	0.001	0.998	1.001	—	0.001	—	1.002
02	43.31	0.40	0.02	55.87	—	0.09	—	99.69	0.987	0.010	0.001	0.998	0.998	—	0.004	—	1.002
03	43.84	0.23	0.03	55.51	—	0.10	—	99.71	0.996	0.005	0.001	1.002	0.994	—	0.004	—	0.998
Rammelsbergite-1 (Fig. 3)																	
04	26.18	1.75	0.15	70.35	—	0.74	—	99.17	0.929	0.062	0.006	0.997	1.955	—	0.048	—	2.003
05	24.60	3.87	0.13	70.25	—	1.38	—	100.23	0.856	0.134	0.005	0.995	1.917	—	0.088	—	2.005
09	25.42	3.91	0.21	68.62	—	1.58	0.45	100.18	0.888	0.134	0.008	1.030	1.859	—	0.100	0.011	1.970
Rammelsbergite-2 (Fig. 6)																	
07	27.88	1.04	0.05	67.42	3.99	0.05	0.32	100.77	0.999	0.037	0.002	1.038	1.882	0.069	0.004	0.008	1.962
08	28.01	0.38	0.01	72.74	0.26	0.39	—	101.79	0.974	0.013	—	0.988	1.983	0.004	0.025	—	2.012
Nickelskutterudite-1 (Figs. 3, 9B)																	
15	19.60	0.79	0.17	78.92	—	0.03	—	99.51	0.948	0.038	0.008	0.994	2.990	—	0.016	—	3.006
13	17.76	2.60	0.27	79.48	—	0.11	—	100.22	0.854	0.124	0.014	0.992	2.998	—	0.010	—	3.008
11	17.35	3.02	0.54	79.51	—	0.39	—	100.81	0.827	0.143	0.027	0.997	2.968	—	0.035	—	3.003
12	17.20	3.60	0.54	78.70	—	0.58	—	100.62	0.818	0.171	0.026	1.015	2.934	—	0.051	—	2.985
10	16.15	3.95	0.33	78.41	—	0.32	—	99.16	0.783	0.191	0.017	0.991	2.981	—	0.028	—	3.009
14	15.58	4.20	0.71	78.09	—	0.64	—	99.22	0.752	0.202	0.036	0.990	2.953	—	0.057	—	3.010

Notes: Dash means that the element has not been detected or has been below detection limit. Numbers of analyses correspond to those in the figures.

Table 2. Chemical composition of nickelskutterudite-2, skutterudite-2, and Fe-skutterudite-2

No anal.	Element, wt %							Formulae normalized on the basis of 4 atoms									
	Ni	Co	Fe	As	Sb	S	Se	Total	Ni	Co	Fe	Total	As	Sb	S	Se	Total
									cat.							anions	
Sharply zoned crystals of nickelskutterudite-2 - skutterudite-2 (Figs. 6, 7)																	
17	19.19	2.09	0.40	78.59	—	0.10	0.33	100.70	0.917	0.099	0.020	1.037	2.943	—	0.009	0.012	2.963
18	18.69	1.99	0.54	80.31	—	0.09	0.13	101.76	0.876	0.093	0.027	0.996	2.989	—	0.008	0.005	3.002
19	17.89	2.62	0.83	79.88	—	0.09	0.12	101.43	0.844	0.123	0.041	1.007	2.980	—	0.008	0.004	2.992
20	15.71	4.77	0.82	79.65	0.08	0.32	0.12	101.46	0.741	0.223	0.040	1.004	2.963	0.002	0.028	0.004	2.996
16	11.24	6.94	1.56	77.95	0.07	0.38	0.41	98.56	0.605	0.332	0.079	1.016	2.934	0.002	0.033	0.015	2.984
21	9.87	9.17	1.75	76.23	0.14	1.21	—	98.37	0.476	0.442	0.089	1.007	2.884	0.002	0.107	—	2.993
22	7.45	12.06	1.97	78.70	0.31	1.40	—	101.89	0.347	0.560	0.096	1.003	2.871	0.007	0.119	—	2.997
23	5.92	12.95	1.88	77.00	0.14	1.89	—	99.78	0.281	0.610	0.093	0.984	2.851	0.002	0.163	—	3.016
Skutterudite-2, Fe-skutterudite-2, and nickelskutterudite-2 overgrowing sharply zoned crystals																	
nickelskutterudite-2 - skutterudite-2 (Figs. 7, 9A)																	
24	14.58	5.99	0.77	79.32	—	0.66	0.11	101.43	0.681	0.279	0.038	0.998	2.937	—	0.056	0.004	2.997
25	6.99	12.44	0.86	77.23	0.09	1.58	—	99.19	0.337	0.598	0.044	0.979	2.880	0.002	0.139	—	3.021
26	7.46	11.70	2.02	78.19	0.02	1.58	—	100.97	0.349	0.546	0.100	0.995	2.869	0.001	0.135	—	3.005
27	7.25	11.97	2.84	77.64	0.20	1.44	—	101.34	0.342	0.516	0.141	0.999	2.873	0.004	0.124	—	3.001
28	6.81	11.83	2.95	77.41	0.22	1.27	0.09	100.58	0.325	0.515	0.148	0.988	2.894	0.005	0.111	0.002	3.012
29	4.73	13.22	3.39	76.67	0.38	1.62	—	100.01	0.223	0.622	0.168	1.013	2.838	0.009	0.140	—	2.987
30	7.22	13.07	0.63	76.67	0.02	1.67	0.15	99.43	0.343	0.619	0.032	0.994	2.855	0.001	0.145	0.005	3.006

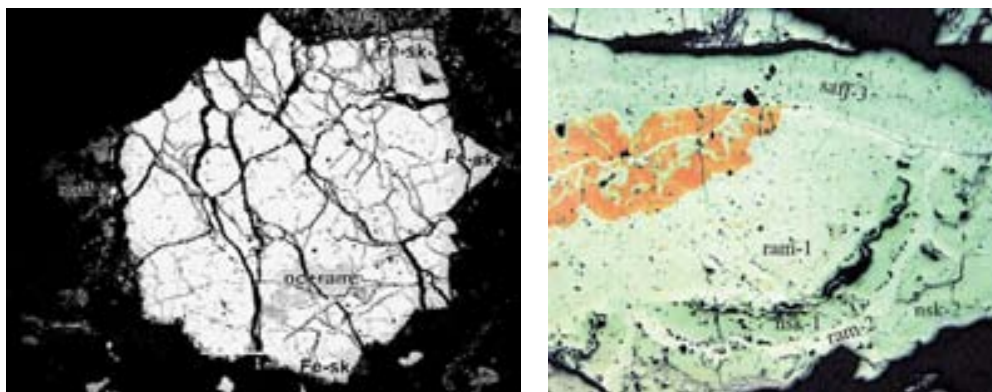


Fig. 4. BSE image of intergrowth of cubic crystals of nickelskutterudite-2 and skutterudite (white). Outer zones are Fe-skutterudite-2 (light grey, Fe-sk-2); relic niccolite in rammelsbergite (grey, nc+ram) in the intergrowth. The generation-3 assemblage of dolomite (black) and Fe-safflorite (dark grey, saff-3) surrounds the large intergrowth.

Fig. 5. Photomicrograph of relations between the three generations of rammelsbergite, nickelskutterudite and safflorite. Relic niccolite (pink) in rammelsbergite-1 (ram-1) and nickelskutterudite-1 (nsk-1). Rim of rammelsbergite-2 on nickelskutterudite-1 followed by zoned crystals of nickelskutterudite-2 (nsk-2). Segregation of rammelsbergite and nickelskutterudite of generations 1 and 2 is overgrown by safflorite-3 (saff-3) and Co-rammelsbergite-3. Polished section. Width of image is 15 mm.

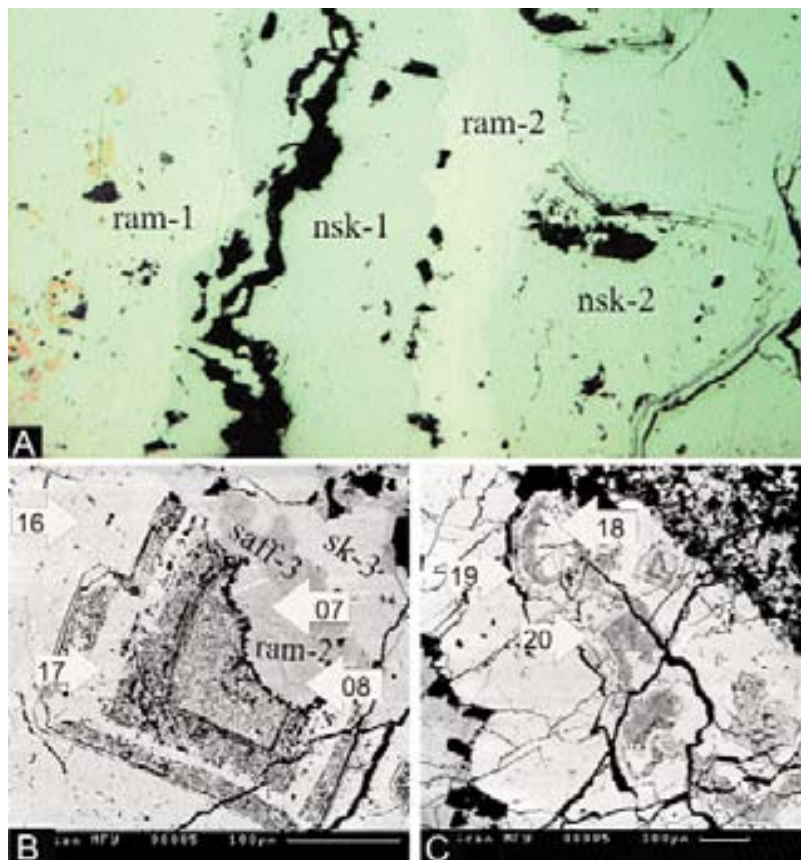


Fig. 6. Intergrowths of three generations of rammelsbergite, nickelskutterudite and safflorite.

A) Photomicrograph of rammelsbergite-1 (ram-1) with relic niccolite (pink) overgrown by nickelskutterudite-1 (nsk-1) with the rammelsbergite-2 rim (ram-2), which is substrate for zoned crystals of nickelskutterudite-2 (nsk-2). Polished section, width of image is 5 mm.

B) BSE image of zoned crystal of Co-nickelskutterudite-2 (white, analyses 16 and 17) has overgrown split rammelsbergite-2 (ram-2, analyses 07 and 08). This is fragment of the generation-2 arsenides overgrown by the generation 3 arsenides safflorite (saff-3) and Ni-skutterudite (sk-3).
 C) BSE image of zoned crystals of nickelskutterudite-skutterudite-2 (grey white, analyses 18–20).

and dolomite have compromise growth surface. This is the first generation of the 8th mineral assemblage.

Rammelsbergite-1 is moderately low in S and Fe-free and contains up to 4 wt % Co and 0.5 wt % Se (Table 1). Nickelskutterudite-1 is low in Co and Fe (Table 1) and shows strong negative correlations between Ni and Co ($r = -0.96$) and Ni and Fe ($r = -0.80$) and strong positive correlations between Co and Fe ($r = +0.75$) and Co and S ($r = +0.70$) ($n = 14$).

Arsenides of generation-2. Generation-1 segregations are overgrown by complex zoned aggregates of generation-2 di- and triarsenides. Relic niccolite-free crystals of rammelsbergite-2 (Figs. 5, 6A, 6B) are overgrown by zoned cubic and cuboctahedral crystals of nickelskutterudite-2 with outer zones of Co-nickelskutterudite-2 and skutterudite-2 (Figs. 5–8, Table 2), which are followed by relatively homogeneous skutterudite-2 with thin zones of Fe-skutterudite-II (Fig. 9A, Table 2). Separate cuboctahedral crystals and intergrowths (up to 5 mm across) of generation-2 triarsenides are observed; Fe-skutterudite-2 is frequently dominant in the outer zones of such grains (Fig. 4).

Rammelsbergite-2 is low in S, moderately low in

Fig. 7. BSE image of aggregation of safflorite-3 (analyses 31–36), dolomite and Co-rammelsbergite-3 (analyses 37 and 38) split crystals, which have overgrown aggregate of the nickelskutterudite – skutterudite-3 (grey-white, analyses 18–24) zoned crystals. Diarsenides are overgrown by Ni-skutterudite (white, analyses 52 and 53) and calcite (black).

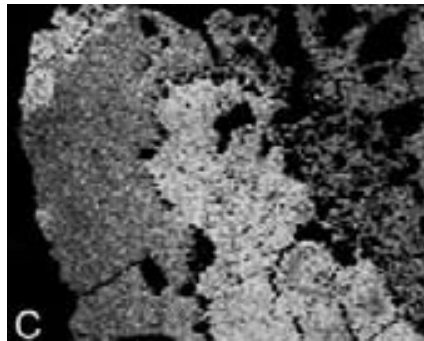
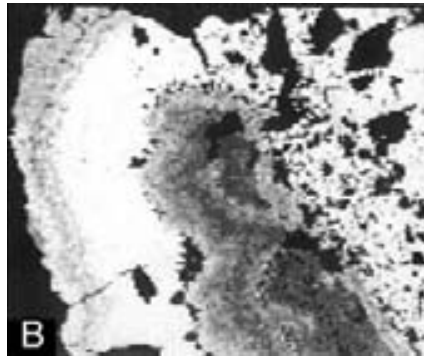
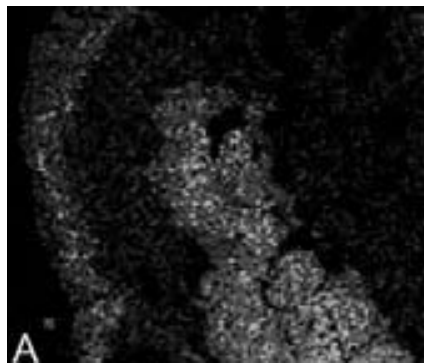
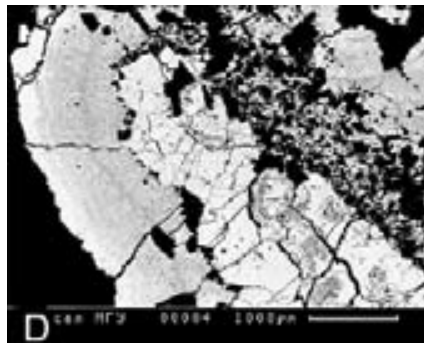
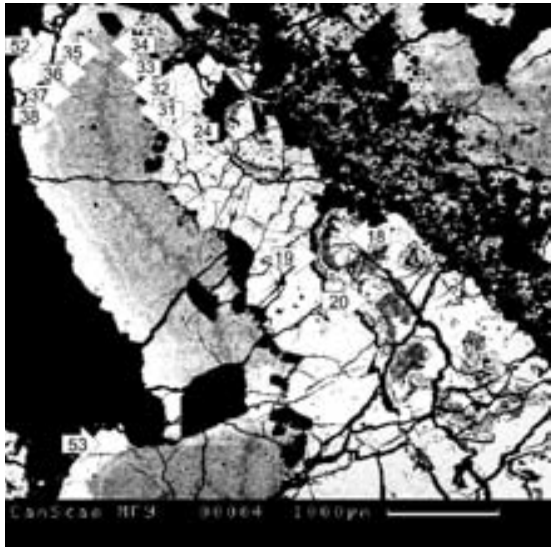
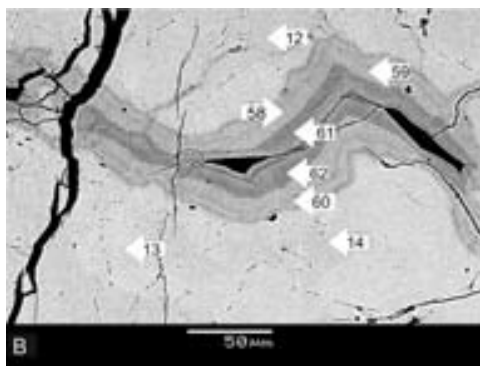
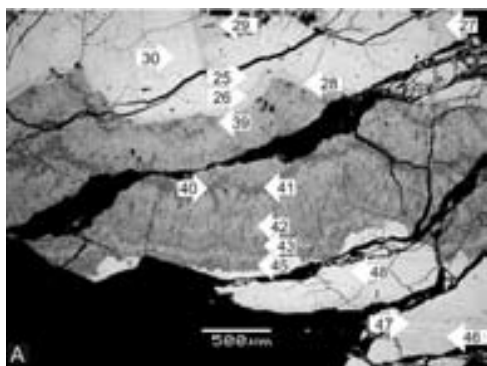
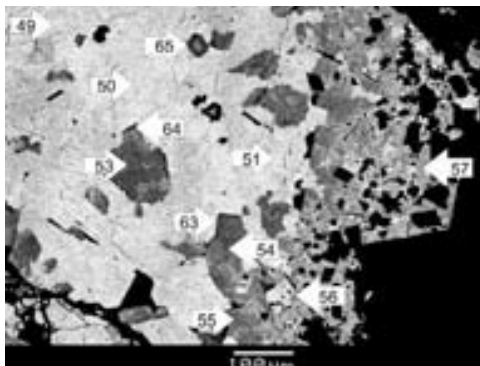


Fig. 8. Aggregation of nickelskutterudite – skutterudite-3, safflorite-3, and Co-rammelsbergite-3. Maps of Ni (A), Co (B), and As (C) distribu-





tion; D) BSE image.



Sb, and low in Co (Table 1). Zoned triarsenides of generation-2 form a continuous nickelskutterudite-skutterudite series and do not contain significant Sb or Se (trace to 0.4 wt %). The concentration of Fe and S in these minerals increases as the skutterudite component increases (Table 2). Strong negative correlations between Ni and Co ($r = -0.98$) and Ni and Fe ($r = -0.64$) and positive correlations between Co and Fe ($r = +0.51$) and Co and S ($r = +0.97$) ($n = 36$) are characteristic of these triarsenides. Later generation-2 triarsenides are skutterudite enriched in Fe and Ni, and infrequently, nickelskutterudite enriched in Co (Table 2), and contain practically no Sb and Se.

Arsenides of generation-3. Segregations of di- and triarsenides with inclusions of dolomite rhombohedra and arsenide-dolomite segregations of generation-3 overgrow individual crystals and aggregates of generation-1 and generation-2 minerals (Figs. 4-8, 9A), cementing them (Fig. 7) and forming veinlets in them (Fig. 9B). They are also present as separate grains. Segregations of strongly fractured

Fe-safflorite-3, S-rich safflorite-3, Ni-safflorite-3 and Co-rammelsbergite-3 (Figs. 7-9A) are earlier, and are overgrown by compositionally homogeneous nickelskutterudite-3 (Fig. 9A, Table 3). Occasionally, arsenide pseudomorphs after safflorite (Fig. 7) involve skutterudite enriched in Fe and Ni (Table 3, analyses 52 and 53). Numerous small sharply zoned crystals of Fe-skutterudite-3 enriched in Fe with rims of ferroskutterudite-3 (Fig. 10) are included in large areas of nickelskutterudite-3. The same Fe-Co- and Co-Fe-triarsenides form veinlets cross-cutting the generation-1 minerals (Fig. 9B) and overgrowing the latter.

Diarsenides of the generation-3 form the continuous safflorite-rammelsbergite series. As with the triarsenides of generation-2, they are depleted in Sb and Se. Safflorite-3 is enriched in Fe, more frequently in combination with S. In general, there are strong negative correlations between Ni-Co ($r = -0.96$), Ni-Fe ($r = -0.84$), and As-S ($r = -0.98$) and a positive correlation between Co-Fe ($r = 0.66$) ($n = 62$).

The triarsenides of generation-3 commonly are nickelskutterudite depleted in Co and almost

Table 3. Chemical composition of nickelskutterudite-3, Ni-skutterudite-3, and Fe-skutterudite-3

No anal	Element, wt %					Formulae normalized on the basis of 3 atoms											
	Ni	Co	Fe	As	Sb	S	Se	Total	Ni	Co	Fe	Total cat.	As	Sb	S	Se	Total anions
Nickelskutterudite-3 overgrowing safflorite-3 (analyses 46-48, Fig. 9A) and isolated grains (analyses 49-51, Fig. 10)																	
46	19.57	0.90	0.24	78.81	—	0.04	—	99.56	0.948	0.044	0.012	1.004	2.993	—	0.003	—	2.996
47	19.27	1.40	0.33	78.92	—	0.14	—	100.06	0.928	0.067	0.016	1.011	2.977	—	0.012	—	2.989
48	18.86	1.75	0.20	79.01	—	0.38	—	100.20	0.904	0.084	0.100	1.088	2.969	—	0.033	—	3.002
49	17.28	2.96	0.34	78.54	—	0.29	—	99.41	0.836	0.143	0.017	0.996	2.978	—	0.026	—	3.004
50	18.50	2.17	0.24	78.02	—	0.30	—	99.23	0.896	0.105	0.012	1.013	2.960	—	0.027	—	2.987
51	15.98	3.15	1.29	78.81	—	—	—	99.23	0.778	0.152	0.066	0.996	3.004	—	—	—	3.004
Ni-skutterudite-3 overgrowing Co-rammelsbergite-3 (Fig. 7)																	
52	8.03	11.63	1.65	76.55	0.12	1.32	0.15	99.45	0.376	0.542	0.081	1.000	2.879	0.003	0.114	0.005	3.000
53	7.21	11.39	2.37	77.84	0.34	1.48	0.15	100.77	0.336	0.529	0.116	0.981	2.880	0.008	0.126	0.005	3.019
Fe-skutterudite-3 (Figs. 9B 10)																	
54	0.98	10.94	8.36	78.82	0.07	0.33	0.05	99.55	0.047	0.525	0.423	0.995	2.972	0.002	0.029	0.002	3.005
55	0.28	11.56	8.22	78.48	0.09	0.71	—	99.34	0.018	0.552	0.415	0.985	2.951	0.002	0.062	—	3.015
56	6.05	10.13	4.43	77.12	0.41	1.34	—	99.48	0.288	0.481	0.222	0.991	2.882	0.010	0.117	—	3.009
57	2.16	13.66	5.10	76.89	0.08	0.97	0.13	98.99	0.104	0.653	0.257	1.014	2.894	0.002	0.085	0.005	2.986
58	0.59	12.89	7.84	77.70	—	1.55	—	100.57	0.028	0.601	0.386	1.015	2.852	—	0.133	—	2.985
59	0.89	14.22	6.04	77.77	—	1.44	—	100.36	0.042	0.667	0.299	1.008	2.869	—	0.124	—	2.993
60	0.29	13.49	7.54	77.23	0.20	1.23	0.20	100.18	0.014	0.635	0.374	1.023	2.860	0.004	0.106	0.007	2.977

Table 4. Chemical composition of Fe-safflorite-3 and Co-rammelsbergite-3

No anal	Element, wt %					Formulae normalized on the basis of 3 atoms											
	Ni	Co	Fe	As	Sb	S	Se	Total	Ni	Co	Fe	Total cat.	As	Sb	S	Se	Total anions
Profile from contact with the generation 2 triarsenides (Fig.7)																	
31	0.49	25.22	3.37	65.46	0.36	5.64	0.25	100.78	0.027	0.824	0.116	0.968	1.682	0.006	0.338	0.006	2.032
32	1.11	23.12	3.95	67.02	0.32	4.21	0.13	99.86	0.055	0.775	0.139	0.969	1.764	0.005	0.259	0.003	2.031
33	—	22.43	4.99	71.02	0.09	1.22	0.21	99.95	—	0.803	0.182	0.985	1.931	0.002	0.077	0.005	2.015
34	—	24.79	4.48	64.82	0.30	5.73	0.08	100.21	—	0.821	0.156	0.977	1.671	0.005	0.345	0.002	2.023
35	0.19	23.70	5.21	65.56	0.17	5.01	0.14	99.97	0.007	0.787	0.182	0.976	1.712	0.003	0.306	0.003	2.024
36	3.55	21.07	3.64	67.00	0.11	4.29	0.14	99.80	0.123	0.707	0.129	0.959	1.770	0.002	0.265	0.003	2.041
37	17.60	11.38	0.81	65.37	0.09	4.98	0.16	100.38	0.586	0.376	0.028	0.991	1.701	0.001	0.303	0.004	2.009
38	17.49	12.52	0.61	67.95	0.10	3.98	0.10	102.74	0.576	0.410	0.021	1.007	1.750	0.002	0.240	0.002	1.993
Profile from contact with the generation 2 triarsenides (Fig.9A)																	
39	0.02	22.81	5.47	69.16	—	1.48	—	98.94	0.001	0.798	0.202	1.001	1.904	—	0.095	—	1.999
40	0.06	23.22	6.48	65.17	—	4.17	—	99.10	0.002	0.782	0.230	1.014	1.728	—	0.258	—	1.986
41	0.05	27.02	4.04	61.57	—	6.87	—	99.55	0.002	0.878	0.138	1.018	1.572	—	0.410	—	1.982
42	8.73	17.16	2.56	67.55	—	3.28	—	99.28	0.293	0.573	0.157	1.023	1.776	—	0.201	—	1.977
43	15.68	12.66	1.20	65.57	—	4.93	—	100.04	0.523	0.420	0.042	0.985	1.714	—	0.301	—	2.015
44	16.64	11.71	0.61	65.32	—	4.10	—	98.38	0.566	0.397	0.038	1.001	1.743	—	0.256	—	1.999
45	18.16	9.31	0.48	68.89	—	2.43	—	99.27	0.631	0.322	0.018	0.971	1.874	—	0.155	—	2.029

Table 5. Chemical composition of ferroskutterudite

No	Element, wt %					Formulae normalized on the basis of 4 atoms									
	anal.	Ni	Co	Fe	As	S	Total	Ni	Co	Fe	Total	As	S	Total	
														cat.	anions
61	0.05	8.70	12.95	79.43	1.31	102.44	0.002	0.398	0.626	1.026	2.864	0.110	2.974		
62	0.01	7.94	12.63	77.56	1.43	99.57	0.001	0.374	0.628	1.003	2.843	0.124	2.967		
63	0.05	8.04	12.38	77.09	1.39	98.95	0.002	0.381	0.619	1.002	2.877	0.121	2.998		
64	0.10	8.82	10.38	77.96	1.24	98.50	0.005	0.423	0.525	0.953	2.938	0.109	3.047		
65	0.05	8.38	12.09	78.01	1.34	99.87	0.002	0.394	0.600	0.996	2.888	0.116	3.004		

Note: See Figures 9 and 10

Fe-, Sb-, S- and Se-free (Table 3, analyses 46-50). Strong negative correlations Ni-Co ($r = -0.99$), Ni-Fe ($r = -0.83$), and As-S ($r = -0.91$) and positive correlation Co-Fe ($r = +0.76$) and Co-S ($r = +0.93$) ($n = 27$) are characteristic of nickelskutterudite-3. Sb-low skutterudite-3 moderately enriched in S and ranging from Ni-free to moderately enriched in Ni (Table 3, analyses 52–60) is less frequent. Strong negative correlations Ni-Co ($r = -0.83$), Ni-Fe ($r = -0.64$), Co-Fe ($r = -0.72$), and As-S ($r = -0.92$) and strong positive correlation Co-S ($r = +0.81$) ($n = 37$) are characteristic of Fe-rich skutterudite-III.

Ferroskutterudite from carbonate veins

The ferroskutterudite-3 grains range in size from 1 to 40 μm . Relief is high close to skutterudite and safflorite and is higher than nickelskutterudite. Values of VHN_{50} (4 indentations) range from 700 to 1050 kg/mm^2 . The mineral is highly reflective (58–54%), white and isotropic under reflected light. The reflectance spectrum close to skutterudite with the slightly higher R values was measured in air with a WTiC certified standard. Reflectance values ($R\%$) are as follows: 400 nm (57.2), 420 nm (57.6); 440 nm (58.0), 460 nm (58.2), 470 nm (58.2) (COM), 480 nm (58.2), 500 nm (58.0), 520 nm (57.6), 540 nm (57.3), 546 nm (57.2) (COM), 560 nm (56.9); 580 nm (56.4); 589 nm (56.2) (COM), 600 nm (56.0), 620 nm (55.5), 640 (55.2 nm), 650 nm (54.9) (COM), 660 nm (54.7), 680 nm (54.3), and 700 nm (53.8).

Ferroskutterudite-3 contains only traces of Ni, Sb and Se (Table 5). The average composition ($n = 5$) is $(\text{Fe}_{0.600}\text{Co}_{0.394}\text{Ni}_{0.002})_{0.996}(\text{As}_{2.888}\text{S}_{0.116})_{3.004}$ i.e., close to $(\text{Fe}_{0.6}\text{Co}_{0.4})_1\text{As}_3$.

X-ray diffraction data for the cubic triarsenides nickelskutterudite, skutterudite and ferroskutterudite are similar. The X-ray diffraction pattern of ferroskutterudite (Table 6) was

Table 6. X-ray powder diffraction data for ferroskutterudite

l_{hkl}	$d_{\text{hkl}}, \text{\AA}$	$d_{\text{hkl}}, \text{\AA}$	hkl
3	5.8	5.77	110
3	4.10	4.085	200
4	3.34	3.335	211
10	2.585	2.584	310
9	2.182	2.184	321
4	1.928	1.926	411
7	1.829	1.827	420
3	1.744	1.742	332
5	1.667	1.6677	422
7	1.602	1.6023	510
6	1.402	1.4011	530
3	1.364	1.3617	600
2	1.291	1.2918	620

Note: Debye-Scherrer camera, D 57.3 mm, $\text{CuK}\alpha$.

indexed by analogy with skutterudite. The mineral is cubic, space group $Im\bar{3}m$, $a = 8,17(1) \text{\AA}$, $V = 545.34(3) \text{\AA}^3$, $Z = 8$.

Conclusions

1. Di- and triarsenide minerals of the anti-monide-arsenide mineralization in the Norilsk ore field was formed during multiple tectonic movements. Later mineral segregations in this complex overgrow and replace earlier ones and are present as veinlets and matrix breccia in the latter. Dolomite is characteristic of di- and triarsenide intergrowths, whereas calcite occurs in mono- and diarsenide intergrowths.

2. During each generation, Ni-Co diarsenides were deposited earlier than the Ni-Co-Fe triarsenides. Diarsenides form a continuous rammelsbergite-safflorite solid-solution series (Fig. 11).

3. During each generation of the di- and triarsenide mineral formation, nickelskutterudite is

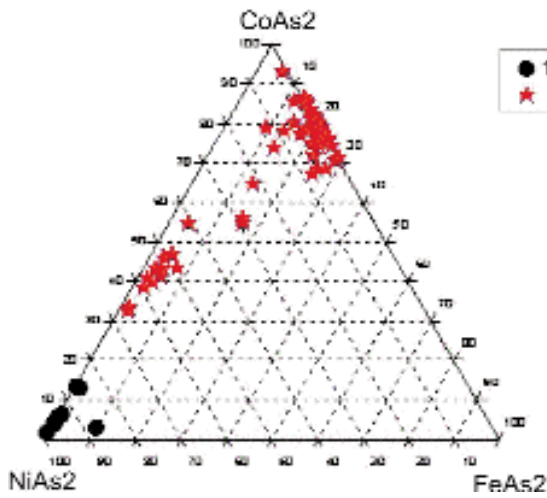
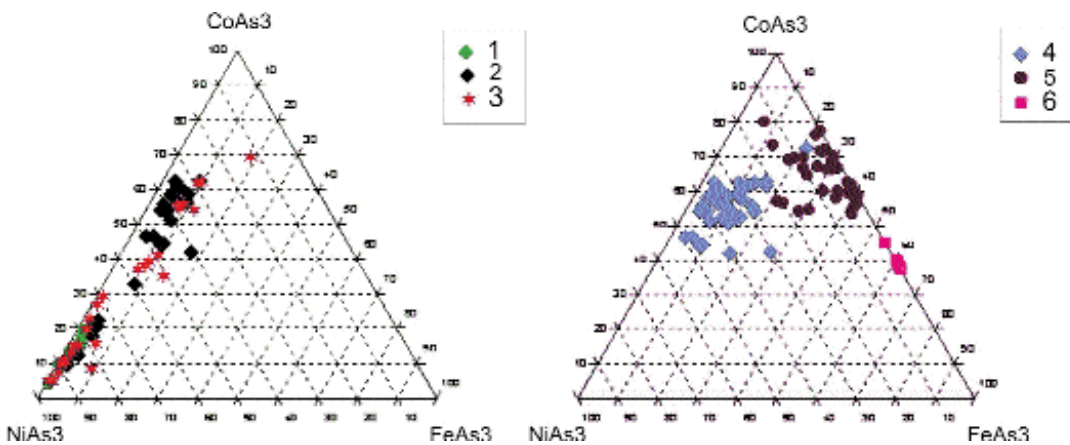


Fig. 9. BSE images of the relations between nickel-skutterudite, Fe-skutterudite, ferroskutterudite and safflorite.

A) Fe-skutterudite-2 (white-grey, analyses 26–30) is overgrown by aggregation of the generation-3 di- and triarsenides: strongly split Fe-safflorite (light grey, analyses 39–42) and Co-rammelsbergite-3 (grey, analyses 43–45) with different S content followed by nickelskutterudite-3 (white-grey, analyses 46–48). Calcite and dolomite are black.

B) Fragment of Fe-skutterudite (grey, analyses 58–60) and ferroskutterudite (dark-grey, analyses 61 and 62) veinlet in nickelskutterudite-1 (light grey, analyses 12–14). Branching calcite veinlets (black).

Fig. 10. BSE images of zoned crystals of ferroskutterudite-3 (dark grey, analyses 63–65) - Fe-skutterudite (grey, analyses 53–57) in nickelskutterudite-3 (white, analyses 49–51). Rhombohedra of dolomite and veinlets of calcite are black.



earlier than skutterudite and Fe-skutterudite.

4. The Norilsk triarsenides form two compositional series in: skutterudite-nickelskutterudite and skutterudite-ferroskutterudite (Fig. 12), characterized by a well-defined negative correlation between Ni and Fe and strong positive correlations between Co and Fe and Co and S.

Acknowledgment

This study was supported by the Russian Foundation for Basic Research (project nos. 04-05-64162 and 07-05-00057).

References

- Distler, V.V., Laputina, I.P., Smirnov, A.V., & Balbin A.S. (1975): Nickel, cobalt, and iron arsenides and sulfoarsenides of the Talnakh ore field //In: Minerals and paragenetic associations of the endogenetic mineral deposits. Nauka, Leningrad (61–74) (in Russ.).
- Dodin, D.A., Batuev B.N., Mitkov G.A., & Izoitko, V.M. (1971): Atlas of Rocks and Ores of the Norilsk Copper-Nickel Deposits. Nedra, Leningrad (in Russ.).
- Fanlo, I., Subias, I., Gervilla, F., Paniagua, A., & Garcia B. (2004): The composition of Co-Ni-Fe sulfarsenides, diarsenides and triarsenides from the San Juan de Plan deposit, central Pyrenees,

- Spain. *Can. Mineral.* 42, 1221–1240.
- Genkin, A.D., Filimonova, A.A., Evstigneeva, T.L. et al. (1981)*: Copper-Nickel Sulfide Ores of the Norilsk Deposits. Nauka, Moscow (in Russ.).
- Godlevsky, M.N. (1959)*: Traps and Ore-bearing Intrusions of the Norilsk District. Gosgeoltekhizdat, Moscow (in Russ.).
- Godovikov, A.A. (1959)*: On dependence of unit-cell dimension of the skutterudite-group minerals on chemical composition //In Proc. Fersman Mineral. Museum 10, 57–73 (in Russ.).
- Gritsenko, Yu.D. & Spiridonov E.M. (2005a)*: Minerals of the continuous rammelsbergite-loellingite and rammelsbergite-safflorite series in the metamorphic hydrothermal antimonide-arsenide-carbonate veins of the Norilsk ore field //Zap. RMO, 134(1), 53–69 (in Russ.).
- Gritsenko, Yu.D. & Spiridonov, E.M. (2005b)*: The niccolite-breithauptite series minerals in ores of the Norilsk district //In: New Data on Minerals, Moscow, Ocean Pictures, vol. 40, 51–64.
- Gritsenko, Yu.D. & Spiridonov, E.M. (2006)*: Nickel, cobalt, and iron sulfoarsenides and sulfoantimonides and krutovite from metamorphic-hydrothermal carbonate veins of the Norilsk ore field //In: New Data on Minerals. Moscow: Ocean Pictures, vol. 41, 46–55.
- Hytönen, K. (1999)*: Suomen Mineraalit. Geologian tutkimuskeskus. Erillisulkaisu.
- Izoitko, V.M. and Vyalov, L.N. (1973)*: On association of the Ni arsenides and antimonides in ores of the Talnakh deposit //In: Minerals and mineral parageneses of ore deposits. Nauka, Leningrad (31–38) (in Russ.).
- Krutov G.A. (1959)*: Cobalt deposits. Gosgeoltekhizdat, Moscow (in Russ.).
- Kulagov, E.A. (1968)*: Mineralogical Features of Ores of the Norilsk-I Deposit //PhD thesis. Moscow State University, Moscow (in Russ.).
- Petruk, W., Harris, D.C., & Stewart, J.M. (1971)*: Characteristics of the arsenides, sulpharsenides, and antimonides. //Can. Mineral. 11, 150–186.
- Radcliffe, D. (1968)*: Structural formula and compositions of skutterudite //Can. Mineral. 9, 559–563.
- Roseboom, E.H. (1962)*: Skutterudites (Co, Ni, Fe)As_{3-x} compositions and cell dimensions //Amer. Mineral. 47, 310–327.
- Rudashevsky, N.S. & Grigor'ev, D.P. (1976)*: Microprobe analysis of the cobalt and nickel tetraarsenides and nomenclature of skutterudite //Zap. VMO. 105(3), 265–281 (in Russ.).
- Rudashevsky, N.S., Shishkin, N.N., and Bud'ko, I.A. (1975)*: Nickel-ore end-member of the CoAs₃–NiAs₃ series //Zap. VMO. 104(2), 209–216 (in Russ.).
- Shishkin, N.N. (1973)*: Cobalt in ores of deposits in the USSR. Nedra, Moscow (in Russ.).
- Schneiderhöhn, H. (1955)*: Erzlagerstätten Kurzvorlesungen zur Einführung und zur Wiederholung. Veb Gustav Fischer Verlag, Jena.
- Spiridonov, E.M., Kulagov, E.A., & Kulikova I.M. (2004)*: Palladium, platinum, and gold assemblages in ores of the Norilsk district //Geol. Ore Depos. 46, 150–165.
- Spiridonov, E.M., Ladygin, V.M., Simonov, O.N., Kulagov, E.A., Sereda, E.V. & Stepanov, V.K. (2000)*: Metavolcanic rocks of the prehnite-pumpelliite and zeolite facies of the trap assemblage, Norilsk region, Siberian Platform. Moscow State University Press, Moscow (in Russ.).
- Vinogradova, R.A. (2002)*: Minerals of nickel and cobalt //Vestn. MSU. Ser. Geol. No. 4, 37–45 (in Russ.).
- Vaughan, D.J. & Craig, J.R. (1978)*: Mineral Chemistry of Metal Sulfides. Cambridge University Press, London.
- Yakovlev, Yu.N., Yakovleva, A.K., & Nera-dovsky, Yu.N. (1981)*: Mineralogy of the copper-nickel sulfide deposits in the Kola Peninsula. Nauka, Leningrad (in Russ.).